

Au/iron oxide catalysts: temperature programmed reduction and X-ray diffraction characterization

G. Neri^a, A.M. Visco^a, S. Galvagno^{a,*}, A. Donato^b, M. Panzalorto^c

^aDepartment of Industrial Chemistry, University of Messina, 98166, Messina, Italy

^bFaculty of Engineering, University of Reggio Calabria, 89100, Reggio Calabria, Italy

^cDepartment of Analytical, Inorganic Chemistry and Molecular Structure, University of Messina, 98166, Messina, Italy

Received 25 August 1998; received in revised form 8 December 1998; accepted 14 December 1998

Abstract

Gold on iron oxides catalysts have been characterized by temperature programmed reduction (TPR) and X-ray diffraction spectroscopy (XRD). The influence of preparation method, gold loading and pretreatment conditions on the reducibility of iron oxides have been investigated. On the impregnated Au/iron oxide catalysts as well as on the support alone the partial reduction of Fe(III) oxy(hydroxides) to Fe₃O₄ starts in the 550 and 700 K temperature range. On the coprecipitated samples, the temperature of formation of Fe₃O₄ is strongly dependent on the presence of gold. The reduction temperature is lowered as the gold loading is increased. The reduction of Fe₃O₄ to FeO occurs at about 900 K and is not dependent on the presence of gold and the preparation method. It is suggested that the effect of gold on the reducibility of the iron oxides is related to an increase of the structural defects and/or of the surface hydroxyl groups. © 1999 Elsevier Science B.V. All rights reserved.

Keywords: TPR; Au/iron oxides catalysts; Iron oxides reduction; XRD

1. Introduction

Gold catalysts supported over metal oxides of the first transition series have been the subject of many recent investigations. These catalysts show an unusual high catalytic activity in the oxidation of CO and H₂ at low temperature [1–3] and in the water gas shift (WGS) reaction [4]. The catalytic performance of Au/iron oxides catalysts in the low temperature CO oxidation has been reported previously [5]. The remarkable enhancement of catalytic activity obtained from the combined effect of gold and the transition metal oxide strictly depends on the method of preparation and on the pretreatment conditions. Au/Fe₂O₃

catalysts prepared by coprecipitation were more active than the impregnated samples [5]. Moreover uncalcined samples have shown a higher initial activity than calcined catalysts.

It seems likely that a metal–support interaction, which is stronger when gold is coprecipitated together with the iron oxide support, is responsible for the enhanced catalytic activity. It is well known that the presence of Au(III) ions influences the nature and the growth of the iron oxides crystallites [6] which in turn can influence the metal–support interaction.

In order to characterize the Au/iron oxides system, a Mössbauer investigation has been carried out and the results are reported elsewhere [7]. Here a temperature programmed reduction (TPR) study on a series of iron oxy(hydroxides) supports and gold/iron oxides cata-

*Corresponding author.

lysts is presented. Samples obtained with different preparation methods, metal loadings and pretreatments conditions have been investigated.

2. Experimental

2.1. Materials

Reagents used were analytical grade. The Au/Fe₂O₃ catalysts were prepared by using HAuCl₄ and Fe(NO₃)₃·9H₂O (Fluka). The gas mixture for TPR experiments was an ultra high purity H₂/Ar (5 vol% of H₂) mixture, purified with molecular sieves and oxygen absorbent traps.

2.2. Sample preparation

Iron oxide samples were prepared by addition of a solution of Fe(NO₃)₃·9H₂O to an aqueous solution of Na₂CO₃ 1 M (pH 11.9) or NaOH 1 M (pH 14) under vigorous stirring (500 rpm) at 7.5 ml/min rate and at temperature between 273 and 348 K. The precipitate was digested overnight at room temperature, washed several times with water and dried under vacuum ($P=10^{-2}$ mbar) at 353 K.

Coprecipitated Au/Fe₂O₃ catalysts were prepared by addition of an aqueous mixture (40 ml) of HAuCl₄ and Fe(NO₃)₃·9H₂O to 400 ml of an aqueous solution of Na₂CO₃ 1 M (pH 11.9) under vigorous stirring (500 rpm) at 7.5 ml/min rate and at a temperature between 273 and 353 K. The gold concentration in the mixture was varied between 2.5×10^{-3} and 10×10^{-3} mol/l whereas the amount of iron was varied between 1.0 and 2.5 mol/l. The coprecipitated sample was kept digesting overnight at room temperature, washed several times with water until free of chloride ions and then it was dried under vacuum ($P=10^{-2}$ mbar) at 353 K.

The impregnated Au/Fe₂O₃ catalyst was prepared by addition, up to incipient wetness, of an aqueous solution of HAuCl₄ (pH 4.3) to iron oxide support. It was then dried under vacuum ($P=10^{-2}$ mbar) at 353 K.

In Tables 1 and 2 are listed the investigated iron oxide and gold samples; details on the preparation conditions and gold analysis of different samples are reported elsewhere [5,7]. In order to make simpler the

Table 1

Main characteristic of iron oxy(hydroxide) samples and quantitative TPR data for the partial reduction of Fe(III) to magnetite

Code	Iron oxide phase	Surface area (m ² /g)	H ₁ /H _{T1}
Fe ₂ O ₃ -A	Hematite ^a	110	1.03
Fe ₂ O ₃ -B	Ferrihydrite ^b	1	0.95
Fe ₂ O ₃ -D ^c	Goethite ^a	35	1.04
Fe ₂ O ₃ -E	Ferrihydrite ^b	15	1.03
Fe ₂ O ₃ -F ^d	Goethite ^a	195	0.99

^aCrystalline phase.

^bAmorphous phase identified by Mössbauer spectroscopy.

^cPrepared at 273 K.

^dPrepared in NaOH 1 M.

Table 2

Main characteristic of Au/Fe₂O₃ samples and quantitative TPR data for the partial reduction of Fe(III) to magnetite

Code	Au (%)	Surface area (m ² /g)	H ₁ /H _{T1}
AF1560/a	15.61	62	0.98
AF017/b	0.17	242	1.03
AF040/b	0.40	269	0.99
AF056/b	0.56	275	0.93
AF117/b	1.17	263	0.92
AF533/b	5.33	246	0.96
AF968/b	9.68	344	1.27
AF578/b ^a	5.78	365	1.10
AF578/b ^{a,b}	5.78	39	0.09
AF578/b ^{a,c}	5.78	51	0.90
AF578/b ^{a,d}	5.78	28	0.98

^aPrepared at 273 K.

^bSample reduced in H₂ at 573 K and exposed to air at room temperature.

^cSample reduced in H₂ at 573 K and reoxidized in air at 573 K.

^dSample reduced in H₂ at 573 K and reoxidized in air at 873 K.

identification, each catalyst has a code indicating the Au content and the preparation method (a=impregnation; b=coprecipitation). Thus for example, AF117/b refers to the coprecipitated sample containing 1.17 wt% of gold.

2.3. Samples characterization

Surface area measurements were made using the BET nitrogen adsorption method in a conventional volumetric apparatus, after outgassing (10^{-4} mbar) the sample at 353 K for 2 h.

X-ray diffraction studies were carried out with a Philips DY 765 diffractometer using the CuK_α radiation. Diffraction peaks of crystalline phases were compared with those of standard compounds reported in the JCPDS Data File.

2.4. Temperature programmed reduction

TPR experiments were carried out in a conventional apparatus. The sample (25–65 mg) was heated from room temperature (RT) to 1073 K (heating rate 10 K/min) under 5% H_2/Ar (vol%), with a constant flow rate of $20 \text{ cm}^3/\text{min}$. A molecular sieve cold trap (maintained at 193 K) and a tube filled with KOH were used to block water and CO_2 , respectively, before the thermal conductivity detector (TCD). The flow rates were monitored by mass flow controllers. The catalysts were heated with a regulated furnace and the temperature was measured by a thermocouple placed inside the catalyst bed. TPR calibration was performed by using a 2% CuO/SiO_2 sample as standard.

3. Results

3.1. Surface area and XRD

Structural characteristics of the samples under study have been investigated by BET surface area (SA) measurements and X-ray diffraction (XRD). The surface areas of the iron oxide samples and of the gold catalysts are reported in Tables 1 and 2, respectively. The iron oxides and the impregnated sample show SA in the range $1\text{--}195 \text{ m}^2/\text{g}$. The SA of coprecipitated catalysts is however much larger; it increases (from 242 to $344 \text{ m}^2/\text{g}$) with increasing the gold loading. The sample AF576/b, obtained by precipitation at lower temperature (273 K), shows the largest surface area ($365 \text{ m}^2/\text{g}$).

On the iron oxide samples the XRD analysis shows the presence of different crystalline iron oxy(hydroxides) phases. This is likely related to the variations in the preparation conditions (precipitating medium, temperature, etc.) of the different samples. The main phases identified on each sample are reported in column 2 of Table 1. On the sample $\text{Fe}_2\text{O}_3\text{-A}$, hematite ($\alpha\text{-Fe}_2\text{O}_3$) is the prevailing crystallographic phase, whereas goethite ($\alpha\text{-FeOOH}$) was found on the $\text{Fe}_2\text{O}_3\text{-$

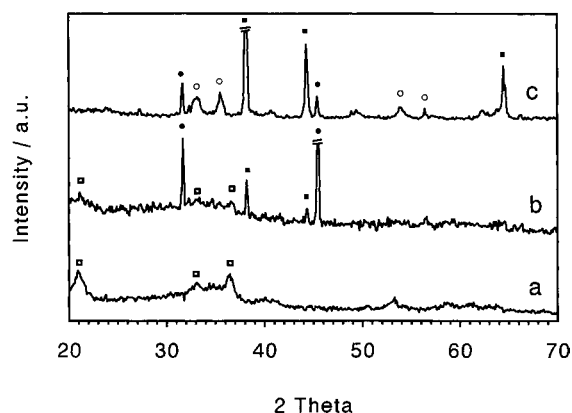


Fig. 1. XRD pattern of: (a) support $\text{Fe}_2\text{O}_3\text{-D}$; (b) sample AF1560/a; (c) sample AF1560/a after treatment with H_2 at 573 K. (●) Unknown phase; (■) metallic gold; (○) hematite; (□) goethite.

D and $\text{Fe}_2\text{O}_3\text{-F}$ samples. The $\text{Fe}_2\text{O}_3\text{-B}$ and $\text{Fe}_2\text{O}_3\text{-E}$ samples show instead an amorphous pattern. The ^{57}Fe Mössbauer analysis of these two latter samples has shown the presence of ferrihydrite ($\text{Fe}_3\text{HO}_8 \cdot 4\text{H}_2\text{O}$) as the main iron phase [7].

Fig. 1 shows the XRD pattern of the impregnated AF1560/a sample (“as prepared” and after reduction in H_2 at 573 K) and that of the parent iron oxide support ($\text{Fe}_2\text{O}_3\text{-D}$). The iron oxide support shows the diffraction peaks of goethite (Fig. 1(a)). On the impregnated catalyst “as prepared” (Fig. 1(b)) it is observed that these peaks have a lower intensity suggesting that the gold precursor interacts with the support decreasing the crystallinity of iron oxide. In addition, the diffraction peaks of metallic gold and two strong reflections at $2\theta = 31.8^\circ$ and 45.6° were also observed. A search on the JCPDS Data File was unable to assign them to known phases of iron or gold. It should be noted that, after reduction at 573 K in H_2 (Fig. 1(c)), these peaks were found to decrease considerably whereas the intensity of the peaks of metallic gold increases. On this basis, it can be suggested that the unknown diffraction peaks observed on the “as prepared” catalyst can be an unidentified gold phase, likely formed by interaction of the gold precursor with the surface of the support. Peaks of minor intensity, related to crystalline hematite, were also found after the thermal treatment and attributed to the transition goethite \rightarrow hematite which is known to occur above 523 K [8].

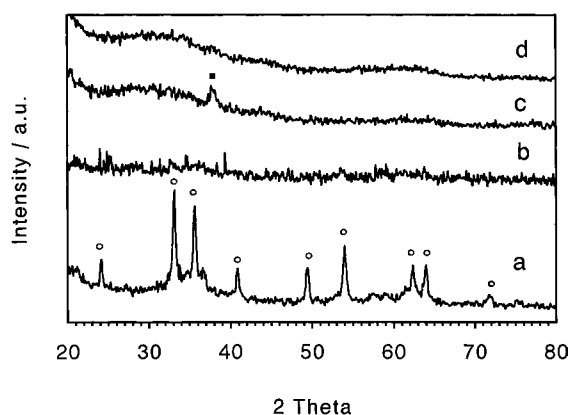


Fig. 2. XRD of coprecipitated samples with different gold loadings: (a) AF040/b; (b) AF117/b; (c) AF533/b; (d) AF968/b. (○) Hematite; (■) metallic gold.

Fig. 2 shows the XRD pattern of some coprecipitated catalysts. At low metal loading a crystalline pattern has been observed (see Fig. 2(a) related to the AF040/b sample). Increasing the amount of gold the crystalline diffraction peaks of iron oxide phases disappear and amorphous spectra have been registered. The most intense diffraction peaks of Au° was observed in the XRD spectra of some samples (Fig. 2(c)). This is in agreement with Mössbauer data which have shown that before thermal treatments the noble metal is mainly present in a oxidized state, but a fraction of metallic gold is also present [7].

Fig. 3 shows the XRD pattern of the AF578/b sample “as prepared” (Fig. 3(a)), after reduction in H_2 at 573 K (Fig. 3(b)) and reoxidation in O_2 at 473 K (Fig. 3(c)) and 873 K (Fig. 3(d)). The “as prepared” sample shows a complete amorphous structure, whereas after treatment in hydrogen the diffraction peaks of magnetite (Fe_3O_4) were found. Metallic gold has been also observed after reduction. The X-ray analysis of the sample after treatment in oxygen at 473 K (Fig. 3(c)) shows that the oxidation of Fe_3O_4 leads to the formation of maghemite ($\gamma\text{-Fe}_2\text{O}_3$). This is revealed by a closer inspection of the spectra (b) and (c) in the range of 2θ between 55° and 65° (see side plot in Fig. 3). Both Fe_3O_4 and $\gamma\text{-Fe}_2\text{O}_3$ have in fact the same spinel-type crystal structure and very similar lattice parameters [9,10]. This also facilitates the conversion from one to the other by a reversible oxidation–reduction reaction. After oxidation at 873 K the diffraction peaks of maghemite and magnetite disappear and the peaks of hematite were found. This is in agreement with the known maghemite \rightarrow hematite transition which occurs at a temperature above 523 K [11].

3.2. TPR

TPR profiles of the iron oxy(hydroxides) samples, listed in order of increasing surface area, are shown in Fig. 4. The TPR profile of the $\text{Fe}_2\text{O}_3\text{-B}$ sample, with a

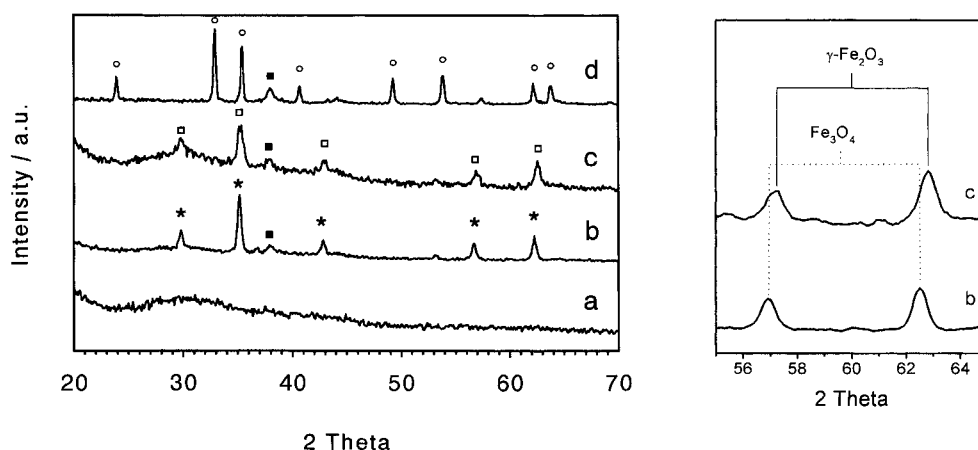


Fig. 3. XRD of sample AF578/b after different pretreatments: (a) sample “as prepared”; (b) after reduction in H_2 at 573 K and exposure to air at room temperature; (c) after reduction in H_2 at 573 K and oxidation in air at 473 K; (d) after reduction in H_2 at 573 K and oxidation in air at 873 K. (○) Hematite; (*) magnetite; (□) maghemite; (■) metallic gold. In the side plot is showed an enlargement of spectra (b) and (c).

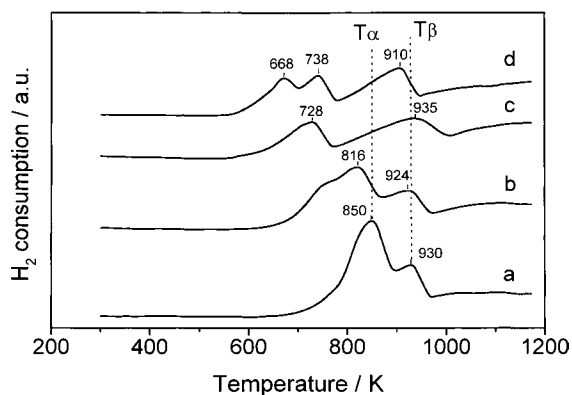


Fig. 4. TPR of iron oxide samples: (a) $\text{Fe}_2\text{O}_3\text{-B}$; (b) $\text{Fe}_2\text{O}_3\text{-E}$; (c); $\text{Fe}_2\text{O}_3\text{-A}$; (d) $\text{Fe}_2\text{O}_3\text{-F}$.

SA of $1 \text{ m}^2/\text{g}$, shows a peak at about 850 K (T_α) and a peak at about 930 K (T_β). Increasing the surface area of iron oxides T_α is shifted to lower temperature; moreover, on the sample with the highest SA T_α was found to split into two peaks. The T_β peak was instead found to be scarcely influenced by the surface area of the iron oxide showing variations not larger than 30 K.

The amount of hydrogen consumed, calculated from the area under the peak T_α , H_1 , (see Fig. 4) corresponds to the reduction of Fe(III) species to magnetite (Table 1). This is outlined from the ratio H_1/H_T , where H_T represents the theoretical amounts of hydrogen which is necessary for the reduction step $\text{Fe(III)} \rightarrow \text{Fe}_3\text{O}_4$. The overall hydrogen consumption calculated by taking in account also the peak T_β corresponds to the formation of wustite, FeO . This was confirmed by XRD which has shown the characteristic diffraction peaks of FeO on a sample reduced up to 930 K. The further H_2 consumption noted at higher temperature and up to 1173 K, where the runs were stopped, can be related to the final transformation of iron oxide(II) into metallic Fe.

The TPR profile of the impregnated AF1560/a catalyst is reported in Fig. 5(a); reduction peaks at 489, 7300 and 916 K have been observed. The peak at 489 K is likely related to the reduction of oxidized gold. The amount of hydrogen consumed corresponds well to the reduction of gold(III) species into metallic gold. TPR of the HAuCl_4 precursor and of Au_2O_3 , are reported for comparison in Fig. 5(c)–(d). The pattern of HAuCl_4 shows a peak at about 554 K whereas the

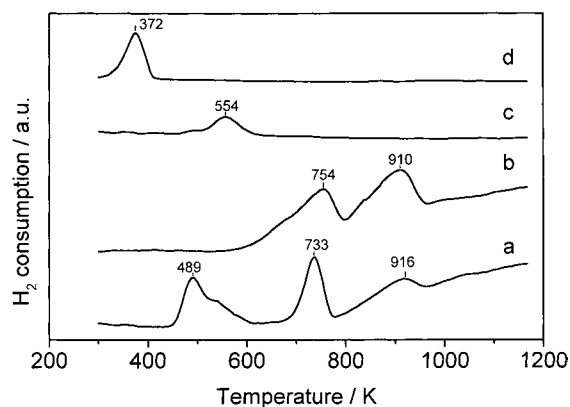


Fig. 5. TPR of: (a) AF1560/a; (b) $\text{Fe}_2\text{O}_3\text{-D}$; (c) HAuCl_4 ; (d) Au_2O_3 .

reduction of gold(III) oxide occur at much lower temperature (372 K). The reduction temperature of gold in the AF1560/a sample is intermediate between that of HAuCl_4 and of gold(III) oxide.

The two peaks at higher temperature in Fig. 5(a) are associated with the T_α and T_β peaks, respectively, observed on the iron oxide samples. A comparison of the TPR pattern of Fig. 5(a) with that of the support alone before impregnation (Fig. 5(b)) shows that, upon addition of gold, the profile of the T_α peak is sharper and shifted to a lower temperature. No significant variations were detected for the reduction peak T_β .

In Fig. 6 are reported TPR profiles of the coprecipitated catalysts having with different gold loading. In

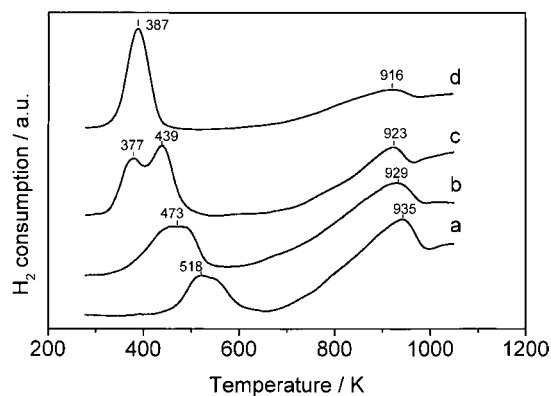


Fig. 6. TPR of coprecipitated catalysts with different gold loadings: (a) AF017/b; (b) AF117/b; (c) AF533/b; (d) AF968/b.

the low temperature region, the pattern of the sample with lower metal loading, AF017/b, show a T_{α} peak starting at a temperature of about 470 K. The hydrogen consumption (Table 2) is in good agreement with the partial reduction of Fe(III) to magnetite. Increasing the gold loading shifts the T_{α} peak to lower temperature. On the sample with the highest metal content the reduction to magnetite starts at a temperature of only 340 K. It can be noted that on these samples (see samples AF578/b and AF1116/b in Table 2) the hydrogen consumed is greater than that necessary for the partial reduction of the support suggesting that the reduction of Au(III) to metallic gold overlaps with that of the support.

The peak (related to the reduction step $\text{Fe}_3\text{O}_4 \rightarrow \text{FeO}$) is always observed at a temperature close to 930 K. As observed on the sample prepared by impregnation, on all coprecipitated samples deviation not higher than 30 K have been noted on the position of T_{β} . This indicates that the formation of FeO is scarcely influenced by the gold content and deposition method.

Fig. 7 show the TPR profiles of the AF578/b sample “as prepared” (Fig. 7(a)) and after reduction and oxidation pretreatments. TPR performed after treatment in flowing H_2 at 573 K and subsequent exposure to air at room temperature shows only a little hydrogen consumption (Fig. 7(b)). After reoxidation with O_2 at 573 K, the subsequent TPR shows in the low tem-

perature range a single peak centred at ~ 429 K. The peak is sharper than that observed on the untreated sample likely due to a more uniform size distribution of the oxide particles after the thermal treatment. When the treatment with O_2 was carried out at higher temperature (823 K) the reduction starts above 550 K (Fig. 7(d)).

4. Discussion

TPR experiments reported in the previous section have shown that the reduction of the iron oxy(hydroxy) phases of the support in the gold catalysts depends strongly on the preparation method, gold content and pretreatment conditions. It is well known that the reduction of bulk iron oxide by hydrogen proceeds through the following steps [12,13]:



Our results agree with this picture and also show that the partial reduction to Fe_3O_4 is favoured on the samples with larger surface area. This is in agreement with the results of Fortuin and co-workers [12] which have reported that the onset temperature of the iron oxide reduction to magnetite depends on the amount of lattice defects. No clear correlation with the nature of iron oxy(hydroxy) phases has been found instead.

The reduction to FeO occurs at about 930 K. Only small variations in the peak position were observed for this reduction step on samples of different surface area.

On the catalyst prepared by impregnation the reduction of the Fe(III) species on the support to Fe_3O_4 and subsequently to FeO, has shown little variations with respect to that observed on the support alone. The reduction of Au(III) species was also clearly observed. It has been noted that the reduction of gold supported species starts at lower temperature in comparison to that observed in the TPR of the HAuCl_4 salt used as precursor. This suggests that in the Au/ Fe_2O_3 system prepared by impregnation more reducible gold species such as Au(III)–oxy(chlorides), formed by interaction of the precursor HAuCl_4 with the surface of iron oxide are presents [14]. Relevant to this it should be noted that on addition of HAuCl_4 to the support, the XRD analysis has shown the formation of an unidentified gold phase which could be responsible for the lower

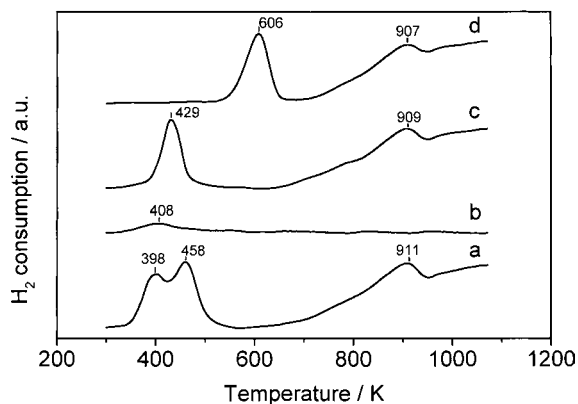


Fig. 7. TPR of sample AF578/b after different pretreatments: (a) Sample “as prepared”; (b) after reduction in H_2 at 573 K; (c) after reoxidation in air at 573 K; (d) after reoxidation in air at 823 K.

reduction temperature observed in the TPR of the impregnated catalyst.

On the coprecipitated catalysts the partial reduction of Fe(III) to magnetite occurs at temperature lower than that reported on the support alone or on the impregnated catalyst. Moreover, a correlation seems to exist between the reduction temperature and the amount of gold on the catalyst. The higher the gold loading, the lower is the reduction temperature. According with these findings, in a recent work on Au/iron oxide Ilieva et al. [15] have reported that in the presence of gold, the reduction step $\text{Fe}_2\text{O}_3 \rightarrow \text{Fe}_3\text{O}_4$ was shifted by ~ 140 K to lower temperature in comparison with $\alpha\text{-Fe}_2\text{O}_3$.

In the same temperature range was found also to occur the reduction of oxidized gold species. As the reduction of gold(III) species occur at temperatures comparable to that of Au_2O_3 this suggests that during the coprecipitation Au(III)–oxy(hydroxy) species can be formed by the hydrolysis of the gold precursor [14].

It should be noted that the BET surface area of coprecipitated samples was very high (>240 m^2/g), even at the lowest metal content (0.17% Au). However, it is not possible to interpret the drastic shift of the reduction temperature of these catalysts only on the basis of a higher surface area.

A recent Mössbauer investigation carried out on similar Au/iron oxide preparations has shown that on increasing the gold content the fraction of ferrihydrite (a highly hydroxylated iron phase) increases [7]. Correspondingly the XRD analysis has shown that the structure of the support on the coprecipitated catalysts become progressively amorphous with addition of gold. Ilieva et al. [15] have reported that on Au/ Fe_2O_3 prepared by coprecipitation the amount of the hydroxyl groups (detected by means of FT-IR and TPD) is higher than that observed on the support alone.

Although we have not performed any relevant experiment, the increase of ferrihydrite with the gold loading could be taken as a proof that the same behaviour occur on our samples. Then, the increase of the structural defects and/or the increase of the amount of surface hydroxyl groups could be considered responsible for the lower temperature of reduction observed on these systems. On this basis the shift to higher temperature of the partial reduction of the

support to magnetite observed on the coprecipitated catalysts after treatment at 823 K, can be explained assuming that such a treatment dehydrates the surface and thereby will deplete the surface concentration of the hydroxyl groups.

It should be noted that, in the absence of gold, ferrihydrite is reduced at very high temperature (see sample $\text{Fe}_2\text{O}_3\text{-E}$). This suggest that gold plays a key role in the reduction of support. The exact mechanism through which it acts is not well understood and deserve further study.

In conclusion, on the basis of the TPR results, the higher activity of coprecipitated samples in comparison to impregnated catalysts can be related to a stronger interaction between gold and iron leading to more reducible species. These species can be assumed to contains much structural defects and/or hydroxyl groups. Taking in account also previous studies on Au/ $\alpha\text{-Fe}_2\text{O}_3$ and Pt/ SnO_x catalysts which have shown that there is a correlation between the concentration of surface hydroxyl groups and the performance of these catalysts [4,15–17] this aspect could be important in order to understand the mechanism of the low temperature CO oxidation and of water gas shift reaction over Au/ Fe_2O_3 catalysts.

Acknowledgements

This work has been carried out with the financial support of MURST.

References

- [1] M. Haruta, S. Tsubota, T. Kobayashi, H. Kageyama, M.J. Genet, B. Delmon, *J. Catal.* 144 (1993) 175.
- [2] S.K. Tanielyan, R.L. Augustine, *Appl. Catal. A* 85 (1992) 275.
- [3] S. Tsubota, A. Ueda, H. Sakurai, T. Kobayashi, M. Haruta, *ACS Symp. Ser.* 552 (1994) 420.
- [4] D. Andreeva, V. Idakiev, T. Tabakova, A. Andreev, R. Giovanoli, *Appl. Catal. A* 134 (1996) 275.
- [5] A.M. Visco, A. Donato, C. Milone, S. Galvagno, *React. Kinet. Catal. Lett.* 61 (1997) 219.
- [6] C. Greffiè, M.F. Benedetti, C. Parron, T. Hiemstra, *C.R. Acad. Sci. Paris* 322 (1996) 197.
- [7] F.E. Wagner, S. Galvagno, C. Milone, A.M. Visco, L. Stievano, S. Calogero, *J. Chem. Soc., Faraday Trans.* 93 (1997) 3403.

- [8] B. Liaw, D.S. Cheng, B. Yang, *J. Catal.* 118 (1989) 312.
- [9] JCPDS Data File 19-0629.
- [10] JCPDS Data File 39-1346.
- [11] K. Siroky, J. Jiresova, L. Hudec, *Thin Solid Films* 245 (1994) 211.
- [12] A.J.H.M. Kock, H.M. Fortuin, J.W. Geus, *J. Catal.* 96 (1985) 261.
- [13] J.W. Geus, *Appl. Catal.* 25 (1986) 313.
- [14] F. Farges, J.A. Sharps, G.E. Brown, *Geochim. Cosmochim. Acta* 57 (1993) 1243.
- [15] L.I. Ilieva, D.H. Andreeva, A.A. Andreev, *Thermochim. Acta* 292 (1997) 169.
- [16] S.D. Gardner, G.B. Hoflund, D.R. Schryer, B.T. Upchurch, *J. Phys. Chem.* 95 (1991) 835.
- [17] D.R. Schryer, B.T. Upchurch, B.D. Sidney, K.G. Brown, G.B. Hoflund, R.K. Herz, *J. Catal.* 130 (1991) 314.